

Leveraging Location Information for RIS-aided mmWave MIMO Communications

Jiguang He, *Member, IEEE*, Henk Wymeersch, *Senior Member, IEEE*, and Markku Juntti, *Fellow, IEEE*

Abstract—Location information offered by external positioning systems, e.g., satellite navigation, can be used as prior information in the process of beam alignment and channel parameter estimation for reconfigurable intelligent surface (RIS)-aided millimeter wave (mmWave) multiple-input multiple-output networks. Benefiting from the availability of such prior information, albeit imperfect, the beam alignment and channel parameter estimation processes can be significantly accelerated with less candidate beams explored at all the terminals. We propose a practical channel parameter estimation method via atomic norm minimization, which outperforms the standard beam alignment in terms of both the mean square error and the effective spectrum efficiency for the same training overhead.

Index Terms—Atomic norm minimization, location information, millimeter wave MIMO, reconfigurable intelligent surface.

I. INTRODUCTION

Reconfigurable intelligent surfaces (RISs) are expected to play a pivotal role in the millimeter wave (mmWave) multiple-input multiple-output (MIMO) systems with very-low cost and near-zero power consumption [1], [2]. They can be seamlessly incorporated into existing systems and used for maintaining the connectivity when the direct line-of-sight (LoS) path between the base station (BS) and mobile station (MS) encounters blockage, which is commonly seen in mmWave MIMO systems [3]. Similar to point-to-point mmWave MIMO systems, efficient channel state information (CSI) acquisition is challenging [4]–[6]. However, the prior information on the channel parameters, e.g., angles of departure (AoDs) and angles of arrival (AoAs), derived from an external location information system on the MS and environmental objects, can help [7], [8].

In this letter, we study the effect of prior location information on channel parameter estimation and beam alignment in RIS-aided mmWave MIMO systems and evaluate the performance in terms of the mean square error (MSE) and the effective spectrum efficiency (SE). For the channel parameter estimation, we harness rough location information for the design of training beams, followed by atomic norm minimization (ANM) for channel parameter extraction. Different benchmark

J. He and M. Juntti are with Centre for Wireless Communications, FI-90014, University of Oulu, Finland (E-mail: jiguang.he@oulu.fi and markku.juntti@oulu.fi).

H. Wymeersch is with Department of Electrical Engineering, Chalmers University of Technology, Gothenburg, Sweden (E-mail: henkw@chalmers.se).

This work is supported by Horizon 2020, European Union’s Framework Programme for Research and Innovation, under grant agreement no. 871464 (ARIADNE). This work is also partially supported by the Academy of Finland 6Genesis Flagship (grant 318927) and Swedish Research Council (grant no. 2018-03701).

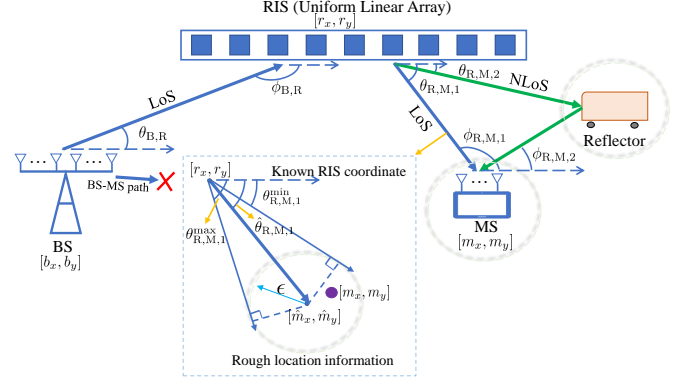


Fig. 1: Coarse location information for RIS-aided mmWave MIMO systems with the direct BS-MS path blocked.

schemes are evaluated to verify the superiority brought by leveraging the prior location information.

II. SYSTEM MODEL

The system model is depicted in Fig. 1, where the direct BS-MS path is blocked and the BS communicates with the MS via the RIS (i.e., BS-RIS-MS path). The BS-RIS channel is assumed to have a single LoS path, denoted as $\mathbf{H}_{B,R} \in \mathbb{C}^{N_R \times N_B}$ with N_B and N_R being the number of antennas at the BS and that of the elements at the RIS, respectively. It can be written as

$$\mathbf{H}_{B,R} = \sqrt{N_B N_R} \rho_{B,R} \boldsymbol{\alpha}_R(\phi_{B,R}) \boldsymbol{\alpha}_B^H(\theta_{B,R}), \quad (1)$$

where the array response vector $\boldsymbol{\alpha}_R(\phi_{B,R}) \in \mathbb{C}^{N_R \times 1}$ is of the form of

$$\boldsymbol{\alpha}_R(\phi_{B,R}) = \frac{1}{\sqrt{N_R}} [1 \ e^{j\pi \sin(\phi_{B,R})} \dots e^{j(N_R-1)\pi \sin(\phi_{B,R})}]^T,$$

with half-wavelength inter-element spacing, $\phi_{B,R}$ and $\theta_{B,R}$ are the AoA and AoD associated with the BS-RIS channel, $\rho_{B,R}$ is the propagation path gain, and $j = \sqrt{-1}$ is the imaginary unit. Similar to $\boldsymbol{\alpha}_R(\phi_{B,R})$, $\boldsymbol{\alpha}_B(\theta_{B,R}) \in \mathbb{C}^{N_B \times 1}$ can be formulated in the same manner.

Without loss of generality, we assume that the BS antenna array is parallel to the RIS and no orientation exists at the RIS. Relying on the geometric relationship between the two terminals, we can calculate the angular values, as

$$\theta_{B,R} = \arccos((r_x - b_x) / \|\mathbf{r} - \mathbf{b}\|_2), \quad (2)$$

$$\phi_{B,R} = \pi - \theta_{B,R}, \quad (3)$$

where $\mathbf{b} = [b_x, b_y]^T$ and $\mathbf{r} = [r_x, r_y]^T$ are the coordinates of the BS and RIS, respectively.

The RIS-MS channel $\mathbf{H}_{R,M} \in \mathbb{C}^{N_M \times N_R}$ with N_M being the number of antennas at MS, is assumed to have multiple resolvable paths in general. Therefore, it is modeled as one LoS path plus a finite number of non-line-of-sight (NLoS) paths, but the NLoS paths are much weaker compared to the LoS path. The RIS-MS channel is in the form of

$$\mathbf{H}_{R,M} = \sqrt{N_R N_M} \mathbf{A}_M(\phi_{R,M}) \text{diag}(\rho_{R,M}) \mathbf{A}_R^H(\theta_{R,M}), \quad (4)$$

where $\mathbf{A}_M(\phi_{R,M}) \triangleq [\alpha_M(\phi_{R,M,1}), \dots, \alpha_M(\phi_{R,M,L_{R,M}})]$, and $\mathbf{A}_R(\theta_{R,M}) \triangleq [\alpha_R(\theta_{R,M,1}), \dots, \alpha_R(\theta_{R,M,L_{R,M}})]$, with $\alpha_M(\cdot) \in \mathbb{C}^{N_M \times 1}$ denoting the array response vector at the MS. The pair of real angles associated with LoS are calculated by following the coordinates of the RIS and MS, similar to (2)–(3) for the BS-RIS channel. We assume that the orientation is known at the MS and its effect can be easily compensated for with fixed offset angle equal to the known orientation. Other pairs of angles rely on the geometric relationship among the reflecting and scattering points in the environment, the RIS, and the MS.

Finally, we assume to have imperfect *a priori* location information of the MS and environmental objects, e.g., from satellite navigation or indoor positioning technology. We model $\hat{\mathbf{m}} = [\hat{m}_x, \hat{m}_y]^T = \mathbf{m} + \mathbf{e}$ with $\mathbf{m} = [m_x, m_y]^T$ being the true coordinate of the MS, where the estimation error \mathbf{e} is upper bounded as $\|\mathbf{e}\|_2 \leq \epsilon$ (see Fig. 1). The location accuracy is characterized by $\epsilon \geq 0$. The potential range for the AoD of LoS path in the RIS-MS channel is

$$\left[\underbrace{\hat{\theta}_{R,M,1} - \arcsin(\epsilon/\hat{d}_{R,M})}_{\theta_{R,M,1}^{\min}}; \underbrace{\hat{\theta}_{R,M,1} + \arcsin(\epsilon/\hat{d}_{R,M})}_{\theta_{R,M,1}^{\max}} \right], \quad (5)$$

where $\hat{d}_{R,M} = \|\mathbf{r} - \hat{\mathbf{m}}\|_2$. Similarly, based on the relationship between $\hat{\theta}_{R,M}$ and $\hat{\phi}_{R,M}$ in (3), the potential range for the AoA of LoS path in the RIS-MS channel is

$$[\pi - \hat{\theta}_{R,M,1} - \arcsin(\epsilon/\hat{d}_{R,M}); \pi - \hat{\theta}_{R,M,1} + \arcsin(\epsilon/\hat{d}_{R,M})]. \quad (6)$$

The potential ranges for the angular parameters related to the NLoS paths of the RIS-MS channel are calculated in the same manner. These ranges are presumed to be computed at the MS and broadcast to the RIS and BS.

III. LOCATION-BASED TRAINING BEAMS

The training beams used at the RIS and MS are generated based on the prior information on the potential angular ranges (5)–(6). Ideally, the group of generated beams used at the RIS should cover the whole potential angular range, where the associated objects (e.g., MS, scatterers, reflectors) may locate. The same principle is applied to the MS. The process is summarized as follows [9]:

- Uniformly quantize the spatial frequency interval $[-1; +1]$ into discrete bins $\{-1 + \frac{1}{M}, -1 + \frac{3}{M}, \dots, 1 - \frac{1}{M}\}$, with $M > \{N_R, N_M\}$; Construct an over-complete dictionary $\mathbf{A}_k = [\alpha_k(-1 + \frac{1}{M}), \alpha_k(-1 + \frac{3}{M}), \dots, \alpha_k(1 - \frac{1}{M})]$ for $k \in \{R, M\}$.
- Determine the spatial frequency range from the available imperfect location information, e.g., $f \in [a; b]$, where $-1 \leq a \leq b \leq 1$;

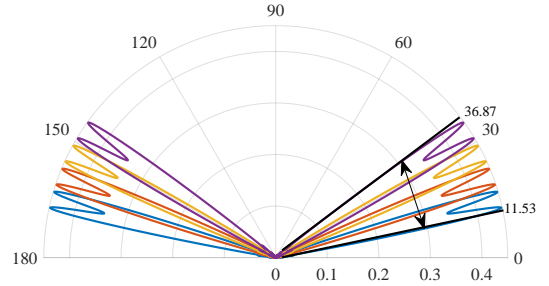


Fig. 2: Training beam design based on the prior information on the angular parameters. Each beam is supposed to have uniform response on certain interval while null response on the rest. In this example, we use 4 beams to cover the spatial frequency range $[0.2 \ 0.6]$, which is calculated based on the rough location information on the MS or environmental objects.

- Suppose we want to cover the interval $[a; b]$ with N beams. We solve $\mathbf{A}_k^H \mathbf{F}_k = \mathbf{G}_k$, for $k \in \{R, M\}$ for $\mathbf{F}_k \in \mathbb{C}^{N_k \times N}$, where $\mathbf{G}_k \in \{0, 1\}^{M \times N}$ is binary matrix with circular shift property, in order to make the designed beam have unit response in a certain interval¹ while null response in the remaining. \mathbf{F}_k can be obtained by the method of least squares (LS) as $\hat{\mathbf{F}}_k = [\mathbf{A}_k]^\dagger \mathbf{G}_k$, with $(\cdot)^\dagger$ denoting the matrix pseudo-inverse. The spatial frequency spanned by one beam is roughly $(b - a)/N$.
- Each column of $\hat{\mathbf{F}}_k$ is regarded as a training beam, used during the channel parameter estimation or beam alignment process. For the RIS, each entry in $\hat{\mathbf{F}}_R$ needs to be constant-modulus in order to satisfy the hardware constraint. Thus, we project each generated beam to the constant-modulus vector space.

An example for the designed beams at the MS is depicted in Fig. 2. Other possible beam codebook designs [10] are left for our future study.

IV. CHANNEL PARAMETER ESTIMATION VIA ANM

The beamforming gain (or effective SE) will be limited by the resolution of the designed beams (according to Section III) in the beam alignment process, proven by the results of one benchmark scheme in Section V. Therefore, we resort to ANM based channel parameter estimation to obtain a refinement (higher-resolution than directly provided by the designed beams) of the channel parameters. This enables a better MS combiner and RIS phase control design compared to the ones chosen from the training beam codebooks.

A. Observation Model

During the training process, the beamformer at the BS is designed based on the known coordinates of the BS and RIS, and the BS steers directly towards the RIS. That is, the beamformer at the BS is fixed as $\mathbf{f} = \alpha_B(\theta_{B,R})$. Assume T different RIS phase control matrices $\mathbf{\Omega}_t$ (with diagonal elements chosen

¹The number of “1” in each column is $\lceil \frac{b-a}{N} / \frac{2}{M} \rceil = \lceil \frac{(b-a)M}{2N} \rceil$. For instance, for the first column of \mathbf{G} , we have $[\mathbf{G}_k]_{\lceil (a+1)/\frac{2}{M} \rceil : \lceil (a+1)/\frac{2}{M} \rceil + \lceil \frac{(b-a)M}{2N} \rceil - 1, 1} = 1$, and the rest of $[\mathbf{G}_k]_{:,1}$ are 0’s.

from the columns of $\hat{\mathbf{F}}_R$, studied in Section III) are taken into consideration with P combining beams \mathbf{w}_p used at the MS (chosen from the columns of $\hat{\mathbf{F}}_M$, studied in Section III), the received signal matrix $\mathbf{Y} \in \mathbb{C}^{P \times T}$ during the training phase are summarized as

$$\mathbf{Y} = [\mathbf{W}^H \mathbf{H}_{R,M} \Omega_2 \mathbf{H}_{B,R} \mathbf{f}_s, \dots, \mathbf{W}^H \mathbf{H}_{R,M} \Omega_T \mathbf{H}_{B,R} \mathbf{f}_s] + \mathbf{W}^H \mathbf{Z}, \quad (7)$$

where s is the transmitted symbol and set to be 1, $\mathbf{W} = [\mathbf{w}_1, \dots, \mathbf{w}_P]$ contains P beams, exploited at the MS, and \mathbf{Z} is the additive noise at the MS with each entry following $\mathcal{CN}(0, \sigma^2)$. \mathbf{Y} can be further expressed as

$$\mathbf{Y} = \sqrt{N_B N_R \rho_{B,R}} [\mathbf{W}^H \mathbf{H}_{R,M} (\boldsymbol{\omega}_1 \circ \boldsymbol{\alpha}_R(\phi_{B,R})), \dots, \mathbf{W}^H \mathbf{H}_{R,M} (\boldsymbol{\omega}_T \circ \boldsymbol{\alpha}_R(\phi_{B,R}))] + \mathbf{W}^H \mathbf{Z}, \quad (8)$$

where $\boldsymbol{\omega}_t = \text{diag}(\boldsymbol{\Omega}_t)$, for $t = 1, \dots, T$, recall that $\boldsymbol{\omega}_t$ is chosen from the columns of $\hat{\mathbf{F}}_R$, and \circ denotes the Hadamard product.

B. Case 1: Only LoS Path from RIS to MS ($L_{R,M} = 1$)

In this case, the RIS-MS channel has only a LoS path. The received signal associated with one training beam pair (one at the RIS, and one at the MS) can be expressed as

$$\begin{aligned} [\mathbf{Y}]_{l,k} &= \xi \mathbf{w}_l^H \boldsymbol{\alpha}_M(\phi_{R,M}) \boldsymbol{\alpha}_R^H(\theta_{R,M}) (\boldsymbol{\omega}_k \circ \boldsymbol{\alpha}_R(\phi_{B,R})) + [\mathbf{W}^H \mathbf{Z}]_{l,k} \\ &= \xi \mathbf{w}_l^H \boldsymbol{\alpha}_M(\phi_{R,M}) \boldsymbol{\omega}_k^T (\boldsymbol{\alpha}_R^*(\theta_{R,M}) \circ \boldsymbol{\alpha}_R(\phi_{B,R})) + [\mathbf{W}^H \mathbf{Z}]_{l,k} \\ &= \xi \mathbf{w}_l^H \boldsymbol{\alpha}_M(\phi_{R,M}) \boldsymbol{\omega}_k^T \boldsymbol{\alpha}_R(\theta_{\text{diff}}) + [\mathbf{W}^H \mathbf{Z}]_{l,k} \\ &= \xi \mathbf{w}_l^H \boldsymbol{\alpha}_M(\phi_{R,M}) \boldsymbol{\alpha}_R(\theta_{\text{diff}})^T \boldsymbol{\omega}_k + [\mathbf{W}^H \mathbf{Z}]_{l,k}, \end{aligned}$$

where $\xi = N_R \sqrt{N_B N_M \rho_{B,R} \rho_{R,M}}$, $\theta_{\text{diff}} \triangleq \text{asin}(\sin(\phi_{B,R}) - \sin(\theta_{R,M}))$. The channel estimation problem is equivalent to LoS channel parameter estimation with prior angular/frequency information. We reformulate the received signal matrix as

$$\mathbf{Y} = \mathbf{W}^H \tilde{\mathbf{H}} \bar{\boldsymbol{\Omega}} + \mathbf{W}^H \mathbf{Z}, \quad (9)$$

where $\tilde{\mathbf{H}}$ is a rank-one channel matrix, as

$$\tilde{\mathbf{H}} = \xi \boldsymbol{\alpha}_M(\phi_{R,M}) \boldsymbol{\alpha}_R^T(\theta_{\text{diff}}), \quad (10)$$

and $\bar{\boldsymbol{\Omega}} = [\boldsymbol{\omega}_1, \dots, \boldsymbol{\omega}_T]$. The low-complexity decoupled ANM [11] is exploited to estimate the AoA of RIS-MS channel and angular difference associated with the RIS. By defining $\bar{\mathbf{U}} = \tilde{\mathbf{H}} \bar{\boldsymbol{\Omega}}$ as $\bar{\mathbf{U}} = \boldsymbol{\alpha}_M(\phi_{R,M}) \bar{\mathbf{c}}$ with $\bar{\mathbf{c}} = \xi \boldsymbol{\alpha}_R^T(\theta_{\text{diff}}) \bar{\boldsymbol{\Omega}}$, the estimation of $\phi_{R,M}$ based on \mathbf{Y} can be formulated as regularized denoising,

$$\min \frac{\mu}{2} \|\bar{\mathbf{U}}\|_{\mathcal{A}_M} + \frac{1}{2} \|\mathbf{Y} - \mathbf{W}^H \bar{\mathbf{U}}\|_F^2, \quad (11)$$

where $\|\bar{\mathbf{U}}\|_{\mathcal{A}_M}$ is the atomic norm of $\bar{\mathbf{U}}$ with the atomic set as $\mathcal{A}_M = \{\boldsymbol{\alpha}(\phi) \mathbf{c}^T \in \mathbb{C}^{N_R \times T} : \phi \in [-\pi; \pi], \|\mathbf{c}\| = 1\}$, and μ is regularization parameter. More details on the estimation of $\phi_{R,M}$ can also be found in [4]. Similarly, we can estimate the angular difference θ_{diff} in the same manner based on \mathbf{Y}^T .

C. Case 2: RIS-MS Multi-path Channel ($L_{R,M} > 1$)

Recall \mathbf{Y} in (8), the (l, k) th entry of \mathbf{Y} is in the form of

$$\begin{aligned} [\mathbf{Y}]_{l,k} &= \mathbf{w}_l^H \sqrt{N_R N_M} \mathbf{A}_M(\phi_{R,M}) \text{diag}(\boldsymbol{\rho}_{R,M}) \mathbf{A}_R^H(\boldsymbol{\theta}_{R,M}) \\ &\quad \times \rho_{B,R} \sqrt{N_B N_R} \boldsymbol{\Omega}_k \boldsymbol{\alpha}_R(\phi_{B,R}) + [\mathbf{W}^H \mathbf{Z}]_{l,k} \\ &= \xi \mathbf{w}_l^H \mathbf{A}_M(\phi_{R,M}) \text{diag}(\boldsymbol{\rho}_{R,M}) \mathbf{A}_R^H(\boldsymbol{\theta}_{R,M}) (\boldsymbol{\alpha}_R(\phi_{B,R}) \circ \boldsymbol{\omega}_k) \\ &\quad + [\mathbf{W}^H \mathbf{Z}]_{l,k} \\ &= \xi \mathbf{w}_l^H \mathbf{A}_M(\phi_{R,M}) \text{diag}(\boldsymbol{\rho}_{R,M}) \mathbf{A}_R^H(\boldsymbol{\theta}_{\text{diff}}) \boldsymbol{\omega}_k + [\mathbf{W}^H \mathbf{Z}]_{l,k}, \end{aligned}$$

where $\boldsymbol{\theta}_{\text{diff}} \triangleq \text{asin}(\sin(\boldsymbol{\theta}_{R,M}) - \sin(\phi_{B,R}) \cdot \mathbf{1})$, where $\mathbf{1}$ is an all-one vector.

This is equivalent to rank- $L_{R,M}$ (rank-deficient) mmWave MIMO channel estimation, and decoupled ANM can also be applied [4].

V. SIMULATION RESULTS

We evaluate the channel parameter estimation performance and effective SE with prior location information. We set $N_B = N_R = N_M = 16$, $\rho_{B,R} \sim \mathcal{CN}(0, 1)$ for all the simulations. The signal-to-noise ratio (SNR) is defined as $1/\sigma^2$. For the channel parameter estimation, we introduce the benchmark where \mathbf{W} and $\boldsymbol{\omega}_i$ are randomly designed. For the effective SE evaluation, two different benchmark schemes (beam alignment) are considered: 1) multiple high-resolution beams used at the RIS and MS [12]; 2) a single wide beam used at the RIS and MS [8]. For 1), we choose the beam pair associated with the highest received signal power. For 2), a wide beam covering the whole potential spatial frequency range is considered and thus no training overhead is consumed. The effective SE is expressed as

$$R = \mathbb{E} \left[\frac{T_c - T_t}{T_c} \log_2 \left(1 + \frac{|\mathbf{w}^* \mathbf{H}_{R,M} \boldsymbol{\Omega}^* \mathbf{H}_{B,R} \mathbf{f}|^2}{\sigma^2} \right) \right] \text{ b/s/Hz},$$

where T_c is the duration of coherence time, T_t is the duration for training, \mathbf{w}^* and $\boldsymbol{\Omega}^*$ are the designed MS combiner and RIS phase control matrix based on the parameter estimates [4].

In the first experiment, we compare the channel parameter estimation with prior location information and that without it, where only a LoS path is considered for $\mathbf{H}_{R,M}$ and $\rho_{R,M} \sim \mathcal{CN}(0, 1)$. The potential spatial frequency range (one-to-one correspondence with the angular range) determined by the rough location information is $[0.2; 0.6]$. Without the location information, the training beams are randomly generated. As shown in Fig. 3, the performance in terms of MSE of channel parameter estimation can be improved significantly with the availability of the MS location information, though it is rough. Also, we provide the theoretical Cramér–Rao lower bound (CRLB) for the angular parameters as a reference for the proposed scheme.²

We evaluate the effective SE with only a LoS path for $\mathbf{H}_{R,M}$, taking into consideration of benchmark schemes 1) and 2). As shown in Fig. 4, the performance can be further improved by estimating the channel parameter, based on which a refinement on the MS combiner and RIS control matrix is achieved.³

²The two curves are aligned with each other, so we only keep one here in the figure.

³Throughout the paper, we assume a single RF chain at the MS, so $T_t = PT$.

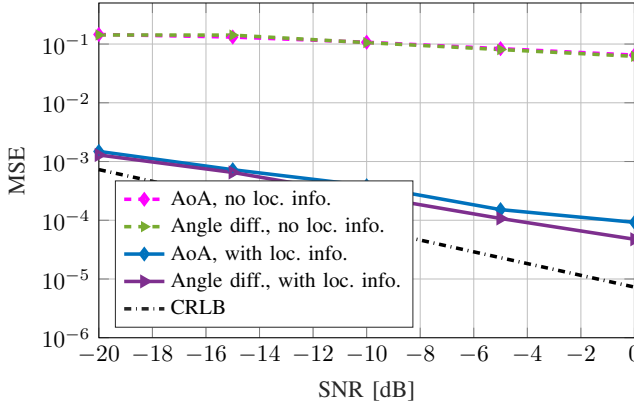


Fig. 3: Angular difference and AoA of $\mathbf{H}_{R,M}$ estimation with $P = T = 4$, $N_B = N_R = N_M = 16$, $L_{R,M} = 1$.

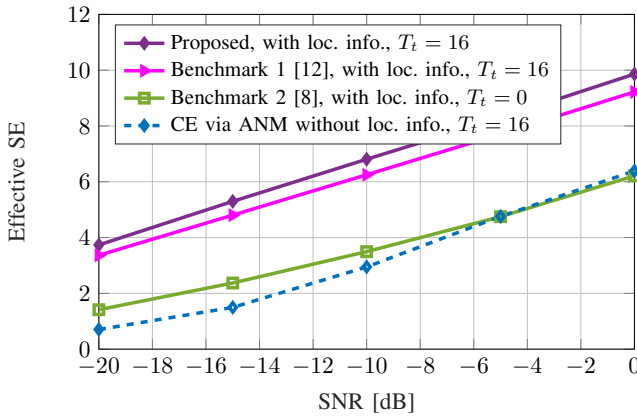


Fig. 4: The effective SE with location information for the single-path scenario.

Now, we extend the study to multi-path scenario for $\mathbf{H}_{R,M}$ with $\rho_{R,M,1} \sim \mathcal{CN}(0,1)$ and $\rho_{R,M,2} \sim \mathcal{CN}(0,0.1)$, and evaluate the channel parameter estimation and effective SE. In this scenario, the potential spatial frequency ranges are set as $[0.2; 0.6]$ and $[0.7; 0.9]$. From the simulation results in Figs. 5 and 6, we can observe that the performance can also be improved significantly by taking the rough location information into consideration.

VI. CONCLUSIONS

We have exploited prior information on the location of the MS and environmental objects in RIS-aided mmWave MIMO systems. It has been verified that the introduction of such prior information can further enhance the performance, e.g., MSE, effective SE, compared to the beam alignment approach.

REFERENCES

- [1] C. Huang, S. Hu, G. C. Alexandropoulos, A. Zappone, C. Yuen, R. Zhang, M. Di Renzo, and M. Debbah, "Holographic MIMO surfaces for 6G wireless networks: Opportunities, challenges, and trends," *IEEE Wireless Communications*, pp. 1–8, 2020.
- [2] M. D. Renzo, M. Debbah, D. T. P. Huy, A. Zappone, M. Alouini, C. Yuen, V. Sciancalepore, G. C. Alexandropoulos, J. Hoydis, H. Gacanin, J. de Rosny, A. Bounceur, G. Lerosey, and M. Fink, "Smart radio environments empowered by reconfigurable AI meta-surfaces: an idea whose time has come," *EURASIP J. Wireless Comm. and Networking*, vol. 2019, p. 129, 2019.

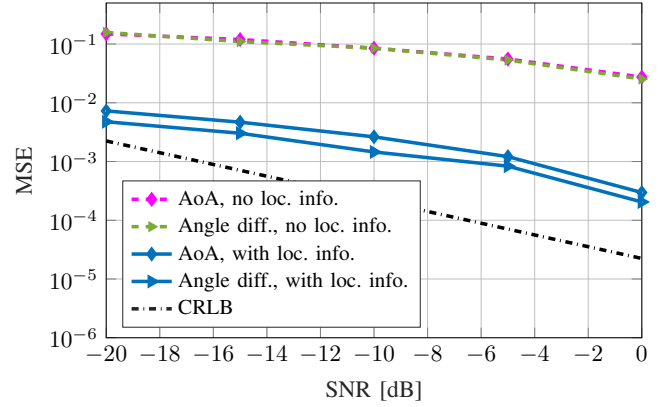


Fig. 5: Angular difference and AoA of $\mathbf{H}_{R,M}$ estimation with $P = T = 8$, $N_B = N_R = N_M = 16$, $L_{R,M} = 2$.

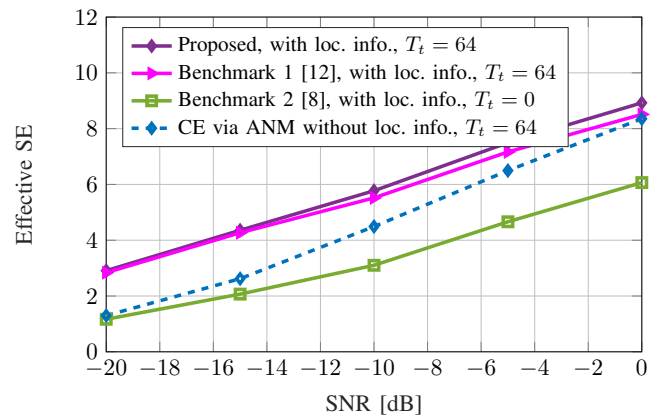


Fig. 6: The effective SE with location information for the multi-path scenario.

- [3] T. Bai and R. W. Heath, "Coverage and rate analysis for millimeter-wave cellular networks," *IEEE Trans. Wireless Commun.*, vol. 14, no. 2, pp. 1100–1114, 2015.
- [4] J. He, H. Wymeersch, and M. Juntti, "Channel estimation for RIS-aided mmwave MIMO systems via atomic norm minimization," *arXiv*, 2020.
- [5] K. Ardah, S. Gherekhloo, A. L. F. de Almeida, and M. Haardt, "TRICE: An efficient channel estimation framework for RIS-aided MIMO communications," *arXiv*, 2020.
- [6] P. Wang, J. Fang, H. Duan, and H. Li, "Compressed channel estimation for intelligent reflecting surface-assisted millimeter wave systems," *IEEE Signal Process. Lett.*, vol. 27, pp. 905–909, 2020.
- [7] G. C. Alexandropoulos, "Position aided beam alignment for millimeter wave backhaul systems with large phased arrays," in *2017 IEEE 7th International Workshop on Computational Advances in Multi-Sensor Adaptive Processing (CAMSAP)*. IEEE, 2017, pp. 1–5.
- [8] N. Garcia, H. Wymeersch, E. G. Ström, and D. Slock, "Location-aided mm-wave channel estimation for vehicular communication," in *proc. of IEEE International Workshop on Signal Processing Advances in Wireless Communications (SPAWC)*, 2016, pp. 1–5.
- [9] A. Alkhateeb, O. El Ayach, G. Leus, and R. W. Heath, "Channel estimation and hybrid precoding for millimeter wave cellular systems," *IEEE J. Sel. Topics Signal Process.*, vol. 8, no. 5, pp. 831–846, 2014.
- [10] W. Wang, W. Zhang, and J. Wu, "Optimal beam pattern design for hybrid beamforming in millimeter wave communications," *IEEE Trans. Veh. Technol.*, vol. 69, no. 7, pp. 7987–7991, 2020.
- [11] Z. Zhang, Y. Wang, and Z. Tian, "Efficient two-dimensional line spectrum estimation based on decoupled atomic norm minimization," *Signal Processing*, vol. 163, pp. 95 – 106, 2019.
- [12] S. Hur, T. Kim, D. J. Love, J. V. Krogmeier, T. A. Thomas, and A. Ghosh, "Millimeter wave beamforming for wireless backhaul and access in small cell networks," *IEEE Trans. Commun.*, vol. 61, no. 10, pp. 4391–4403, 2013.